Nickel activation for hydrogenolysis reaction on USY zeolite

Luciana Tavares dos Santos[a], Marcelo Hawrylak Herbst[b], and Marcelo Maciel Pereira[a,*]

[a] *Departamento de Química Inorgânica, Instituto de Química, Centro de Tecnologia, A-628, Universidade Federal do Rio de Janeiro, Rio de Janeiro, RJ, Brazil, 21945-970*

[b] *Departamento de Física dos Sólidos, Instituto de Física, Centro de Tecnologia, 68528, Universidade Federal do Rio de Janeiro, Rio de Janeiro, RJ, Brazil, 21945-970*

Received 23 September 2003; accepted 4 November 2003

The effects of the SAR (14 and 38) and of the methodology of introduction of nickel (wetness impregnation and ion exchange) on catalyst activation were investigated in Ni/USY model catalysts submitted to two activation treatments: reduction (A) and reduction/calcination/reduction, successively (B). For the catalysts prepared by wetness impregnation, a marked increase in the catalytic activity after treatment B was observed. On the basis of the catalyst efficiency toward ethane hydrogenolysis, the lower SAR catalyst presents a threefold higher activity. On the contrary, the catalysts prepared by ion exchange, as well as a model catalyst prepared by wetness impregnation over a USY exhaustively exchanged with nickel ions, do not present measurable increasing of the catalytic activity under the same activation conditions. Monitoring the catalyst activation by EXAFS indicates the formation of nickel clusters in the impregnated catalysts after activation treatment B, which should be responsible for the high catalytic activity. However, TEM images reveal a bimodal particle size distribution, with large (ca. 20 nm) and small nickel particles. Temperature-programmed reduction performed under the same conditions of catalyst activation suggests that only the small nickel particles are activated under the experimental conditions adopted in this work.

KEY WORDS: USY; nickel; EXAFS; ethane hydrogenolysis; TEM.

1. Introduction

The structure and properties of small metallic particles supported on oxides and zeolites continue to attract considerable attention. There is currently great interest in the electronic and catalytic properties of these systems, as well as in the basic processes involved in the formation of stable metallic nanoparticles [1]. In order to understand real catalysts, it is desirable to develop model catalysts for the systematic study of the complex interactions between metallic particles and supports.

Model systems of nickel in micro-, meso- and macroporous supports [2–4] have been continuously studied, but unfortunately most of the research has been done at high nickel content, in contrast with low metal contents usually found in industrial catalytic processes.

Concerning this, the study of model systems with nickel content in the order of parts per million is suitable for understanding the processes involved in the poisoning of FCC catalysts.

The chemical properties of a metal-containing catalyst change significantly as a function of the size of metallic particles, especially in the case of reactions sensible to the structure. Furthermore, it is known that the metallic particle size is not the only parameter responsible for tuning the properties of a catalytic system: the electronic, structural and chemical characteristics of the support usually have great importance in designing a catalyst. Notwithstanding, small metallic clusters dispersed in the surface of an oxide or another support can be more active and selective as catalysts when compared with large metallic particles in the same support [5,6]. As an example, methane decomposition is fairly effective in catalysts containing small nickel particles [7].

However, sintering of metallic particles under reaction conditions is responsible for a considerable efficiency loss of industrial catalysts, and is therefore an important aspect to be considered in the study of metal-containing catalysts [8]. Thus, supported metallic nanoparticles have attracted considerable attention in catalysts development, owing to the high activities they promote in heterogeneous catalytic processes, and also due to the resistance toward sintering presented by these systems. With regard to nickel nanoparticles, Penchev *et al.* [9] proposed that the catalytic activity of nickel is a function of the $1/r_{\text{particle of nickel.}}$

Modeling of real catalytic systems requires preparation methods suitable to the industrial catalyst manufacture. Transition metal ions are usually introduced in the support by ion exchange, wetness impregnation or pH-controlled precipitation. The wetness impregnation method is the most used method to prepare supported nickel catalysts; most of nickel ions are dispersed in the outer surface and comparatively fewer ions are incorporated into the support framework [10].

Recently, the formation of nickel nanoparticles in the mesopores of an MCM41 silica was studied [11]. The catalyst was prepared by impregnation, using nickel citrate as the precursor. According to the authors, there

* To whom correspondence should be addressed.
E-mail: maciel@iq.ufrj.br

1011-372X/04/0100–0081/0

occurs the formation of a film of the nickel chelate over the mesoporous support and, upon calcination, NiO nanoparticles could be observed by transmission electron microscopy (TEM). Reduction treatments showed that the nickel oxide could be converted into metallic nickel nanoparticles without damaging the support. On the other hand, catalysts prepared with nickel nitrate present only a small amount of nanoparticles in the mesoporous phase, and most of nickel is found in the external surface of the MCM41.

Evidence of resistance of nickel nanoparticles toward sintering in zeolites was reported by Bein *et al.* [12]. Nickel was introduced into zeolite Y using $Ni(CO)_4$ as precursor, obtaining a bimodal particle distribution, with cluster size between 0.5 and 1.5 nm, as shown by EXAFS and TEM measurements. Mitsuru *et al.* [13] also characterized nickel exchange in Y-type zeolite by EXAFS, and proposed that after NaOH treatment there occurs the formation of nickel hydroxide-type compounds. After oxidation and reduction treatments, metallic nickel particles were formed in the zeolite.

Particularly on zeolites, the questions associated to the formation of active metallic sites may become very complex: the various possibilities of metal-ion siting and of metallic diffusion through the framework of these systems can lead to complex structural alterations. On the other hand, these characteristics also create the possibility of detailed studies, allowing the control of fundamental properties that may be directed to practical applications.

Currently, a great interest has been focused on the activation of small molecules, such as methane and ethane, for the generation of hydrogen and/or hydrocarbons of higher molecular weight [14]. From the point of view of the catalytic activity of metallic sites, it has been claimed that an augmentation in the electronic density increases the metal–adsorbate interaction [15], and, as a consequence, the greater the electronic delocalization, the lower the activity of the catalyst.

With regard to this, the design of catalytic systems containing small metallic particles supported on zeolites seems to satisfy simultaneously the practical need for efficient catalysts toward the activation of small molecules, and also for the understanding of the fundamental aspects related to metallic clustering in confined environments.

The aim of this letter is to report a suitable method for the activation of nickel in USY model catalysts that favor the formation of small metallic particles active toward ethane hydrogenolysis.

2. Experimental

2.1. Preparation of catalysts

USY zeolite was activated through the ion exchange of Na^+ ions for H^+ ions. A solution of 2M of NH_4NO_3 was used in order to reduce the level of Na_2O in the faujasite. The exchange was carried out at 70 °C for 1 h, and after an intermediate drying at 120 °C for 12 h, a second ion exchange was carried out. The zeolite was calcined in a furnace at 600 °C for 2 h, and the final concentration of Na_2O was 1%. The USY was submitted to a hydrothermal deactivation to modify the SAR. This treatment was carried out in a furnace under the following conditions: temperature = 800 °C; partial pressure of steam = 0.33 atm; flow = 60 mL/min; treatment time = 12 h. The two values of SAR used in this work were 14 (before the treatment) and 38 (after the treatment) [16].

To prepare nickel-zeolite model catalysts, two different methods for introducing the metal were employed. The first was wetness impregnation using nickel carboxylate in toluene as the precursor. The reaction was carried out in a rotary evaporator for 30 min at ambient temperature. The catalyst was dried for 1 h under vacuum at 80 °C and then calcined in a furnace at 600 °C for 2 h. The second method introduced the metal through ion exchange [17] using nickel nitrate. The exchange was carried out in aqueous solution at 70–80 °C, for 2 h. The solution was filtered and washed with 2 L of demineralized water at 65 °C. The catalyst was dried at 120 °C for 12 h and then calcined at 600 °C for 3 h. The nomenclature for the catalysts was standardized as follows: Ni14i (nickel in the SAR14 zeolite introduced by impregnation) and Ni38t (nickel in the SAR38 zeolite introduced by ionic exchange). All catalysts presented Ni concentrations near 0.8 wt/wt%. Additionally, for the sake of comparison, a third catalyst was prepared in which nickel was introduced by impregnation in a previously exhaustively exchanged zeolite of SAR 14 (4 times) with nickel nitrate until attaining a nickel content of 7 wt/wt%, Ni14ti.

2.2. Catalytic tests

The reaction used for characterizing the activity of the supported metallic particles was ethane hydrogenolysis. The catalysts were previously reduced under flow of 60 mL/min of a mixture of 10% H_2/N_2 from ambient temperature to 500 °C (heating rate of 10 °C/min), standing at this temperature for 2 h (treatment A). The temperature of the reactor was lowered to 430 °C and the reaction was performed with a mixture of 10% C_2H_6/H_2 (flow of 20 mL/min). At the end of the reaction, the temperature of the reactor was raised to 600 °C (heating rate of 10 °C/min) and the catalysts were calcined *in situ* under air for 3 h (flow of 60 mL/min). This was followed by an additional reduction step, under the same conditions, and the ethane hydrogenolysis reaction was repeated under the previously described conditions. The complete process, namely, reduction at 500°C/2 h, calcination at 600°C/3 h and reduction at 500°C/2 h carried out *in situ* was called treatment B.

To verify the influence of oxygen on the catalytic activity, the catalysts were submitted, after reduction and before the catalytic test, to a pulse of 5% O_2/Ar, for about 1 min. The products of the reaction, ethane and methane, were analyzed by GC in line (Shimadzu Gc-17a), starting 3 min after the beginning of the reaction and carrying out a total of three injections. The conditions of analysis were the following: column Al_2O_3/KCl (Chrompack), column temperature = 110 °C, detector temperature (FID) = 230 °C and injector temperature = 210 °C. No deactivation was observed.

2.3. EXAFS measurements

EXAFS measurements were carried out at the XAS I beamline at the National Laboratory of Synchrotron Radiation [18] (LNLS, Brazil), operating at 1.37 GeV, with a maximum ring current of 120 mA. The synchrotron radiation beam was monochromated by a Si(220) double crystal. The spectra were collected in the K edge of Ni (8333 eV) in the fluorescence mode, using a Ge multielement detector. In the first stage of the work, the analyses were carried out *ex situ;* where the samples were pressed in the form of pellets, before and after the catalytic reactions, and the XAS spectrum was measured in contact to the ambient. Later, in an attempt to prevent contact with the atmosphere, we developed a strategy that consists in the following: the catalysts were prepared in glass reactors that were sealed under vacuum and transferred to the sample holders in an inert nitrogen atmosphere glove box. For these so-called *in situ* EXAFS measurements, the sample holders were wrapped with Kapton tape and stored under inert atmosphere until the moment of the measurements. The spectra of metallic Ni foil (6 μm) and of NiO powder were also measured as references for data treatment. The XAS spectra were subtracted from background through a polynomial curve, and, after standard data treatment using the WinXAS routine, the FT–EXAFS were compared with the standards, metallic Ni and NiO.

2.4. Temperature-programmed reduction (TPR)

The temperature-programmed reduction (TPR) was performed in a Micromeritics 2900 instrument. The profile was obtained under flow of 30 mL/min of a mixture of 1.7% H_2/Ar, from room temperature up to 500 °C (heating rate of 10 °C/min), standing at this temperature for 2 h. After 2 h, the temperature of the reactor was raised to 600 °C (heating rate of 10 °C/min) and the catalysts were calcined *in situ* under flow of 30 mL/min of a mixture of 5% O_2/He for 3 h. This was followed by an additional reduction step, under the same conditions.

2.5. Transmission electron microscopy (TEM)

The catalysts were characterized using a high-resolution TEM combined with EDX carried out with a Philips CM-30 electron microscope working at 300 kV and equipped with an analytical system link. These measurements were carried out at the University of Barcelona.

3. Results

The results of the catalytic tests, summarized in table 1, show that after treatment A (reduction 500 °C/2 h), low conversion rates are observed for all the catalysts. The catalysts Ni14i and Ni38i achieved a rate of 0.07 and 0.03 mol C_2H_6/min g_{Ni} respectively. After treatment B, a significant increase in the conversion is observed for these catalysts. The measured rates were 13.5 (Ni14i) and 1.3 (Ni38i). In other words, the activation effect is much more evident in the lower

Table 1
Results of catalytic tests in Ni/USY

Catalyst	Mass (g)	Ni content (wt/wt%)	C_{et}% (A)	[b]C_{et}% (B)	Mol C_2H_6/min.gNi (A)	Mol C_2H_6/min.gNi (B)
Ni14i	0.2370	0.82	0.4	76.4	0.07	13.45
Ni14i[b]	0.2210	0.80	0.3	68.1	0.05	12.50
Ni38i	0.2368	0.82	0.2	7.3	0.03	1.25
Ni14t	0.2245	0.67	0	0	0	0
Ni38t	0.2196	0.60	0	0	0	0
Ni14ti	0.2300	0.82	0	0	0	0
Ni/SiO_2	0.1120	1.30	13.0	–	2.90	–
Ni14i[a]	0.2113	0.82	0	28.3	0	5.66
Ni/SiO_2[a]	0.1034	1.30	11.4	–	2.75	–

[a]Catalysts dealt with oxygen.
[b]$C_{et}\% = ((\text{net} - n^{\circ}\text{et})/n^{\circ}\text{et}) * 100$; where n°et is the number of mol/min of ethane fed in the system and net is the unconverted number of mol/min.

SAR catalyst. It is noteworthy that pure zeolites and catalysts prepared by ion exchange did not present any increase in the catalytic activity after this treatment. A catalytic test carried out after a calcination treatment at 600°C/3 h and sequential reduction at 500°C/2 h on the original Ni14i catalyst did not induce any enhancement on its catalytic activity. Furthermore, the method of introduction of nickel seems to have influence in the resulting catalytic activity: the Ni14ti catalyst, in which nickel was introduced by wetness impregnation after the zeolite was exchanged with 7 wt/wt% of Ni, did not present any activity enhancement after treatments A and B.

The effect of oxygen poisoning was investigated over Ni14i and Ni/SiO_2 catalysts. On zeolite-supported nickel, the catalytic activity decreased (rate of 13.5 to 5.7 mol C_2H_6/min g_{Ni}). On the other hand, only a slight decrease was observed for the Ni/SiO_2 catalyst (table 1).

The TPR profile of the Ni14i catalyst did not present any hydrogen consumption after both the first and the second reductions. It is important to emphasize that the catalyst remained at 500 °C under H_2/Ar flow for 2 h. In a previous work [19], we investigated the reducibility of Ni/SiO_2 catalysts. A Ni/SiO_2 catalyst with 7-nm particle size (1.3% Ni, introduced by wetness impregnation) presents only 15% of reduction when submitted to a TPR analysis from room temperature to 500 °C.

The results of the catalytic tests suggest that in Ni/USY catalysts the nickel active sites are somewhat different from those of Ni/SiO_2. In order to investigate the structure of the nickel particles on Ni/USY, EXAFS measurements were performed.

The background-subtracted XAS spectra of the model catalysts are presented in figure 1. It is noteworthy that the XANES spectra of Ni14i after treatment B and of 7% Ni14t are quite similar, even though these catalysts show very different activities toward ethane hydrogenolysis. On the other hand, after treatment A, the XANES spectrum of Ni14i catalyst presents a preedge feature, which resembles the NiO reference and is absent in the spectrum of 7% Ni14t catalyst.

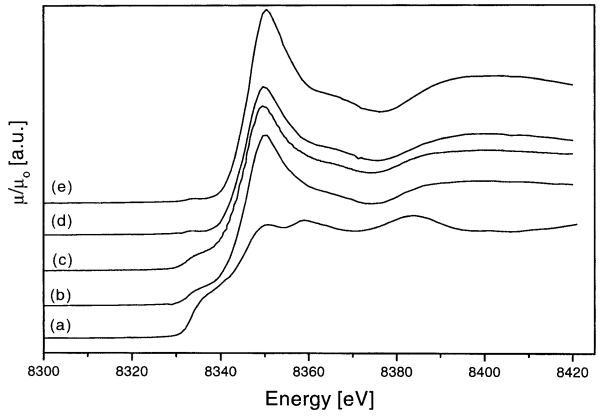

Figure 1. Background-subtracted XAS spectra (a) Metallic nickel, (b) Ni14i after treatment B, (c) NiO, (d) Ni14t after treatment B, (e) Ni14i after treatment A.

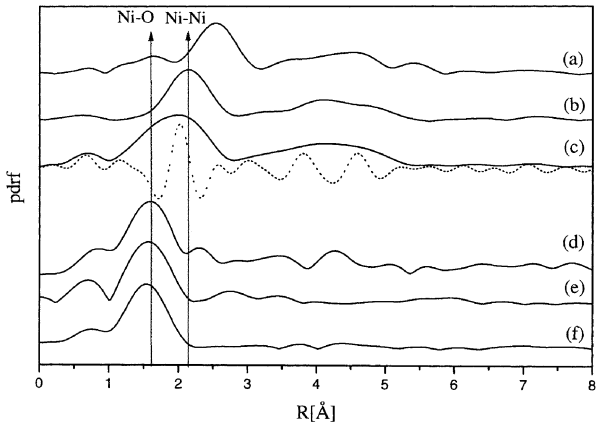

Figure 2. FT–EXAFS of the standards: (a) NiO, (b) Metallic nickel; and of the catalysts prepared *ex situ*, (c) Ni14i after treatment B, (d) Ni38i after treatment B, (e) Ni14i after treatment A, (f) Ni14t after treatment B.

Notwithstanding, Fourier transforms of the EXAFS spectra measured *ex situ* and presented in figure 2 clearly show that metallic particles were formed in the Ni14i catalyst submitted to activation treatment B. In the FT–EXAFS of this catalyst, broad features are observed, suggesting the contribution of both Ni–Ni and Ni–O absorber–scatterer pairs. These contributions are easily observed in the imaginary part of the FT–EXAFS signal, and correlate quite well with the first neighbor radial distance of bulk nickel (~2.1 A) and nickel oxide (~1.6 Å) standards. In the 2.5–5 Å region of the PDRF of the FT–EXAFS, there are also discernible broad features, but the unambiguous assignment to either Ni–Ni or Ni–O higher-order radial distances cannot be done at this stage of data treatment.

On the other hand, the FT–EXAFS of Ni38i submitted to the same activation treatment of Ni14i (treatment B) does not show convincing evidence for the formation of nickel clusters. Strictly speaking, according to the radial distance observed for the main peak of the FT–EXAFS, about 1.6 Å, the formation of a nickel oxide-like phase can be proposed in this catalyst. Interestingly, in the FT–EXAFS of low SAR catalyst

Table 2
Maxima of the FT–EXAFS taken from the spectral deconvolution

Samples	Maxima of peaks (Å)[a]			
NiO	1.21	1.63		2.54
Ni metal			2.16	
Ni14i – A	1.25	1.74		
Ni14i – B		1.50	2.08	

[a] Distances not corrected.

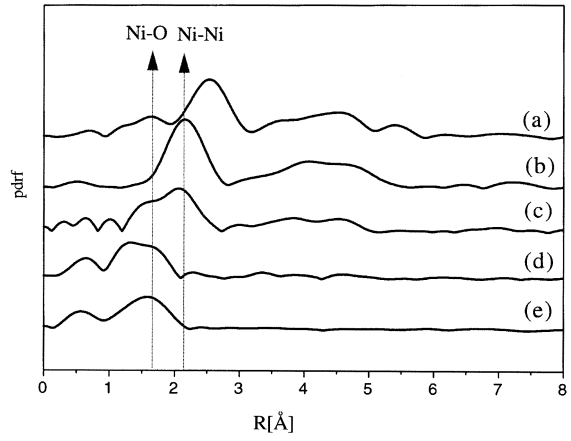

Figure 3. FT–EXAFS of the standards: (a) NiO, (b) Metallic nickel; and of the catalysts prepared *in situ*: (c) Ni14i after Treatment B, (d) Ni14i After Treatment, (e) 7%Ni14t.

Ni14i submitted only to reduction (activation treatment A), and in Ni14t, prepared by ion exchange and submitted to activation treatment B, the same trends already observed in the FT–EXAFS of Ni38i were revealed, perhaps with even less crystallinity of the nickel oxide-like phase, judging from the lower intensities of the higher distance radial peaks.

In order to investigate the origin of the oxygen contribution to the EXAFS signal, the catalysts were analyzed under inert atmosphere, as described in the Experimental section. The results of these so-called *in situ* EXAFS measurements are shown in figure 3. For the Ni14i catalyst prepared according to activation treatment B, the broad peak observed around 2 Å in the *ex situ* FT–EXAFS spectrum now appears to be split into two peaks, whose maxima are slightly shifted to smaller radial distances when compared with the bulk nickel or nickel oxide standards.

It is noteworthy that shifting to lower distances in the FT–EXAFS spectrum is commonly observed in systems composed of nanosize particles. Moreover, the exclusion of atmospheric oxygen leads also to a resolution enhancement in the 2.5–5 Å region of the spectrum. These results suggest that the nickel clusters are very susceptible to oxygen poisoning, as indeed observed in the catalytic tests. On the other hand, and following the same trends already observed in the *ex situ* EXAFS measurements, the catalysts Ni14i activated by treatment A, Ni38i submitted to activation treatment B, and the ion exchanged Ni14t did not show convincing evidence for nickel clustering, even in the experimental conditions of exclusion of atmospheric oxygen.

The catalyst Ni14i was examined by TEM after the treatments A and B. This catalyst does not present Ni particles. On the other hand, after treatment B, the catalyst presents large nickel particles (around 20 nm diameter), figure 4.

4. Discussion

The FT–EXAFS profiles of all catalysts prepared by ion exchange, after treatment B and of the Ni14i catalyst after treatment A are quite similar. However, as previously indicated, the catalytic activity after treatment B is significantly enhanced only for the impregnated catalyst. From the results of the catalytic tests, it is concluded that nickel environments on Ni14i and 7% Ni14t are quite different. According to XANES and EXAFS data, these catalysts share only the first local neighborhood, showing a distance compatible with the Ni–O bonding, but actually the nickel atoms are in different chemical environments. Probably in the impregnated catalyst, after treatment A, most of the nickel is to be found outside of the zeolite framework 20.

It was observed that the variation of catalytic activity is sensitive to the SAR of the catalyst. Generally speaking, a direct relationship between the ion exchanging capability of the framework and the catalytic activity is observed. As stated previously, in this work, we investigated two values of the SAR, 38 and 14, and these catalysts have different activities toward ethane hydrogenolysis; the catalytic activity is inversely proportional to the SAR. This trend is demonstrated by the lack of activity in the Ni14ti catalyst.

The results discussed above support the hypothesis that the USY framework has an important role in the formation of nickel active sites for ethane hydrogenolysis. Moreover, the effect of the extra framework aluminum (EFAL) in cluster formation cannot be disregarded. Notwithstanding, for the sake of comparison, a model catalyst prepared over an HY zeolite with SAR 5, in which EFAL is practically absent, presented a quite similar catalytic behavior of the Ni14i catalyst.

The properties of nickel particles in Ni/USY catalyst and in the previously studied Ni/SiO_2 are quite different. The Ni14i catalyst is more active to the ethane hydrogenolysis and its activity is significantly decreased after oxygen poisoning when compared with Ni/SiO_2 catalyst, although TEM images of both catalysts reveal large nickel particles (20 and 7 nm, respectively). Furthermore, the nickel reducibility in Ni/USY and Ni/SiO_2 catalysts is quite different, as shown by TPR.

These differences observed in Ni/SiO_2 and Ni/USY indicate that sintering of nickel particles on USY is not significant. Thus, according to this result, the active metallic particles in Ni/USY should be smaller than those in Ni/SiO_2.

Although the results suggest the formation of small nickel particles, presumably responsible for the great increasing of activity in the Ni14i catalyst, it was not possible to see those particles by TEM.

Nevertheless, the results of the catalytic activity tests were corroborated by the EXAFS measurements. On comparing the FT–EXAFS for the Ni14i catalyst after

treatments A and B, an increase in the intensity of the nickel–nickel peak is observed up to 4.5 Å in the PDRF, indicating that there is ordering in the next nearest neighbor coordination sphere. Moreover, exposing the catalyst to oxygen at ambient temperature influences in the organization of the nickel particles, but does not lead to a redispersion of the nickel atoms. On the other hand, a broadening of the peak around 2 Å is observed, suggesting the presence of oxygen neighbors with some similarity to nickel oxide.

It should be remembered that the mechanism of formation of the active sites is an element of speculation in the literature. Sintering could occur through the diffusion of small metallic aggregates [21]. Although nickel presents a tendency to form large particles, the formation of small metallic aggregates has already been reported in the literature [22]. A synergism between the zeolite framework and the small clusters, which in fact stabilize the catalyst [10], has been suggested. Nevertheless, the diffusion phenomenon would be favored for metallic nickel nanoparticles in accordance with previously reported result [21].

5. Conclusions

With suitable activation conditions, it was possible to promote a large increase in the activity for ethane hydrogenolysis in Ni/USY catalysts. These catalysts suffer from a severe poisoning when exposed to oxygen, in comparison with a simpler system, Ni/SiO_2. Although the sintering phenomenon is present, as shown by TEM measurements, the high catalytic activity and the susceptibility to oxygen poisoning in Ni/USY catalysts can be justified only if small metallic particles are formed during activation. It was also observed that the silicon–aluminum ratio and compensation ion presented a marked effect on catalytic activity.

Acknowledgments

The authors gratefully acknowledge the Programa de Recursos Humanos da ANP (scholarship to LTS) and the CNPq for a research fellowship (MHH). This research was partially supported by the LNLS – National Laboratory of Synchrotron Radiation, Brazil. We also acknowledge TEM analysis performed at the University of Barcelona.

References

[1] M. Bäumer and H.-J. Freund, Prog. Surf. Sci. 61 (1999) 127.
[2] P. Turlier *et al.*, Appl. Catal. 19 (1985) 287.
[3] R. Burch and A.R. Flambard, J. Catal. 85 (1984) 16.
[4] P.J. Reucroft *et al.*, Appl. Catal. 3 (1982) 65.
[5] M. Haruta, Catal. Today *36 (1997) 153*.
[6] T.C. Campbell, C.S. Parker and E.D. Starr, Science 298 (2002) 811.
[7] E.G.M. Kuijpers *et al.*, J. Catal. 72 (1981) 72.
[8] T.C. Campbell, Surf. Sci. Rep. 227 (1997) 1.
[9] V. Penchev *et al.*, Advan. Chem. Ser. 121 (1973) 461.
[10] V. Pârvulescu and L.B. Su, Stud. Surf. Sci. Catal. 143 (2002) 575.
[11] J.D. Lensveld *et al.*, Stud. Surf. Sci. Catal. 143 (2002) 647.
[12] B. Thomas *et al.*, J. Am. Chem. Soc. 121 (1988) 1801.
[13] S. Mitsuru *et al.*, J. Am. Chem. Soc. 109 (1987) 52.
[14] L. Guczi, R.A Van Santen and K.V. Sarma, Catal. Rev. 38 (2) (1996) 249.
[15] R.A. van Santen, Catal. Lett. 16 (1988) 59.
[16] S.R. Jong *et al.*, Zeolites 6 (1986) 225.
[17] C.R. Moreira, M. Schmal and M.M. Pereira, Stud. Surf. Sci. Catal. 143 (2002) 915.
[18] L.T. Santos, M.H. Herbst and M.M. Pereira, Activity Report LNLS (2002) 118.
[19] L.T. Santos *et al.*, Catal. Today 78 (2003) 459.
[20] L.T. Santos *et al.*, Catal. Today 2853 (2002) 1.
[21] C.H. Bartholomew and W.L. Sorensen, J. Catal. 81 (1983) 131.
[22] L. Bonneviot *et al.*, J. Phys Chem. 90 (1986) 2112.